View metadata, citation and similar papers at core.ac.uk

brought to you by CORE

provided by DSpace at University of West Bohemia

Monitoring of phosphorus cross-contamination in ion implantation of arsenic by spreading resistance profiling and simulations

Marián Kuruc[1], Ladislav Hulényi[2], Rudolf Kinder[2]

[1] ON Semiconductor Slovakia, a.s.,
Vrbovská cesta 2617/102, 921 01 Piešťany, Slovak Republic
E-mail:

[2] Slovak University of Technology, Faculty of Electrical Engineering,
Department of Microelectronics,
Ilkovičova 3, 812 19 Bratislava, Slovak Republic
E-mail: marian.kuruc@onsemi.com, ladislav.hulenyi@stuba.sk, rudolf.kinder@stuba.sk

Anotace:
Při využívaní iontového implantátora pro různé prvky (bór, fosfor, arzén, antimon) může docházet ke kontaminaci nežádoucím prvkem. Zvláštní pozornost je potřebné věnovat zabránění fosforové kontaminaci při implantaci arzénu a antimonu. Uvedená metoda na monitorování úrovně fosforové kontaminace při arzénové implantaci je alternativou k SIMS (Secondary Ion Mass Spectrometry). Tato metoda kombinuje využití simulace a metody odporu šíření SRP (spreading resistance profiling) k určování fosforové kontaminace při arzénové implantaci po difuzním procesu. Monitorování bylo uskutečněno pro vysokodávkovou implantaci arzénu. Pomocí programu SUPREM byl vytvořen teoretický model, který umožňuje určit vliv různých dávek fosforové kontaminace v arzénové implantaci. Tento model byl následně validován pomocí SIMS a SRP měření. Uveden je vliv různých úrovní fosforové kontaminace (až po 10^{14} cm^{-2} dávky fosforu) na profil volných nosičů náboje který byl pozorován při provoze iontového implantátora. Taktéž je uveden konverzní graf, pomocí kterého lze z hloubky p-n přechodu měřeného metodou SRP určit dávku kontaminace fosforem. Experimentální výsledky ukázaly dobrou shodu mezi SIMS daty a navrhovanou SRP metodou. Tato SRP metoda může být použitá pro detekci dávek fosforu až po 10^{12} cm^{-2} a představuje levnější metodu na kontrolu fosforové kontaminace v arzénové implantaci než SIMS.

Abstract:
Cross-contamination with different species can occur when using ion implantation equipment for implantation of various species (boron, phosphorus, arsenic, antimony). Special precaution needs to be taken to prevent phosphorus cross-contamination in implantation of arsenic and antimony**.** An alternative method to Secondary Ion Mass Spectrometry (SIMS) is proposed for monitoring the level of phosphorus cross-contamination in arsenic implantation. This method combines simulations and Spreading Resistance Profiling (SRP) for determination of phosphorus contamination in arsenic implantation after diffusion process. Monitoring of this contamination was done on high dose arsenic implantation. A simulation model was created using SUPREM to estimate the effects of different phosphorus doses in arsenic implantation. This model was validated by SIMS and SRP measurements. The effects of different levels of phosphorus contamination on carrier concentration profiles observed during ion implanter operation are presented (up to 10^{14} cm^{-2} of phosphorus dose). A conversion chart is also presented for conversion of *p-n* junction depths measured by SRP to cross-contamination dose of phosphorus in arsenic implantation. Experimental results have shown good correlation between the proposed SRP technique and SIMS. This SRP method can be used for identification of phosphorus doses as low as 10^{12} cm^{-2} and presents a less expensive method for monitoring of phosphorus cross-contamination in arsenic implantations than SIMS.

INTRODUCTION

Ion implantation became primarily a method for introduction of impurity atoms into the silicon wafer. The main advantages of ion implantation compared to chemical doping process are high accuracy of the desired dose over many orders of magnitude of doping levels and precise control of the depth profiles by controlling the ion implant energy. In ULSI technology boron, phosphorus, arsenic and antimony are most frequently used dopant impurities for BCD technology. In order to better utilize the expensive ion implanter tool, wafer fabs use ion the implanter for implanting multiple elements. However, in this case it is necessary to have proper control of dopant cross-contamination. During normal implanter operations all parts of the implanter that are exposed to the ion beam (beam line, process chamber, disc with wafers) become contaminated with various

dopant species. This cross-contamination mostly occurs in high-current implanter batch-type tools and this effect is also called "implanter memory". Special precaution needs to be taken for phosphorus contamination in arsenic (^{75}As) or antimony (^{121}Sb) implants. If there is phosphorus contamination then it exhibits anomalously high diffusivity in presence of ^{75}As and ^{121}Sb [1] and can diffuse beyond arsenic or antimony profile. In many devices the unwanted and uncontrolled presence of phosphorus would lead to unacceptable variation in the device performance [2]. Dopant cross-contamination is generally produced by these causes: a) sputtering of previously implanted species (e.g. phosphorus) from wheel parts near the wafer, b)evaporation of phosphorus and phosphorus compounds from components receiving the P implant and which are at high enough temperatures to evaporate the phosphorus (e.g. some wheel and beamstop parts) c) sputtering from previously implanted beamline parts, and d) contaminants arising from the ion source not rejected by analysis magnet [3].

In this article we present an alternative method to Secondary Ion Mass Spectrometry (SIMS) for determination of phosphorous (^{31}P) cross-contamination in arsenic (^{75}As) implantation. This method uses Spreading resistance profiling measurements (SRP) and simulations by process simulator SUPREM-IV. In our previous work we have successfully used this method for evaluation of phosphorus contamination in antimony implantations and now we have applied the same principle as described in [4, 5] for determination of phosphorus contamination in arsenic implantation. We present data from monitoring of our implanter for phosphorus contamination in arsenic implantation used for source-drain formation of MOS transistors.

EXPERIMENTAL DATA

For our experiments we have used p-type (Boron) wafers, with 150 mm diameter, thickness 675 μm, crystallographic orientation <111> and resistivity 5 to 15 Ωcm. The wafers were implanted using the high-current batch implanter EATON NV-GSD200. The implant conditions were energy E=75 keV and dose of arsenic N_D(As)= 7.8×10^{15} cm^{-2}. The samples were prepared during three months of standard implanter operation.

For several runs we have prepared multiple samples in one implant batch (presuming the same cross-contamination dose of wafers implanted in one batch) and compared the results obtained by SIMS directly after implantation with SIMS results obtained after diffusion process, and the results from SRP technique. We have also prepared a few samples that were implanted in a different tool that is not used for phosphorus implantations and therefore should be clean of phosphorus (samples Imp7 and Imp8). Another test was done on samples Impl27, Impl28, Impl29, Impl30) where we grew 22nm oxide layer prior ion implantation to protect silicon from contamination and verify efficiency of this layer in prevention of contamination. SIMS profiles ($N_D(x)$) were measured by CAMECA 6F Magnetic Sector SIMS. $N_{c\text{-}SRP}(x)$ profiles were measured using SSM2000 NanoSpreading Resistance Measurement system. Samples were bevelled using 0.1 micron diamond paste on the bevel angle 17'. This provided spatial resolution of 25nm.

The measured $N_D(x)$(P) profiles of phosphorus hidden in arsenic $N_D(x)$(As) profile directly after implantation are shown in Fig. 1. $N_D(x)$(As) profile is shown only for sample Imp18 as it is practically the same for all other samples. These selected samples present a wide range of ^{31}P cross-contamination.

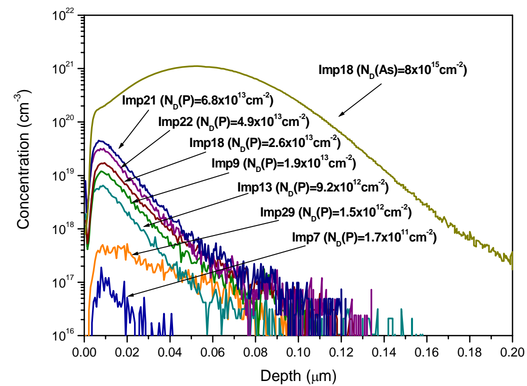

Fig. 1. Selected SIMS $N_d(x)$ profiles for samples showing different levels of ^{31}P cross-contamination in arsenic implantation measured immediately after implantation.

Prior to SRP analysis, the samples were processed by diffusion process to show the effect of phosphorus cross-contamination on the carrier concentration profile. The samples were first covered by deposited oxide (TEOS) to prevent out-diffusion of arsenic. The following diffusion process consisted of 12 hours annealing at T=1050°C in nitrogen atmosphere. After this process the oxide from the samples was etched using 10:1 HF. The diffusion process was selected to drive phosphorus deep enough that it becomes "visible" in the carrier concentration profile ($N_{c\text{-SRP}}(x)$ profile) measured by SRP. Typical $N_{c\text{-}SRP}(x)$ profiles showing different levels of cross-contamination are shown in Fig. 2.

For comparison selected samples were also measured by SIMS after diffusion process. $N_D(x)(P)$ profiles for selected samples are shown on Fig.3. $N_D(x)(As)$ profile is shown only for sample Imp19 as it is practically the same for all other samples.

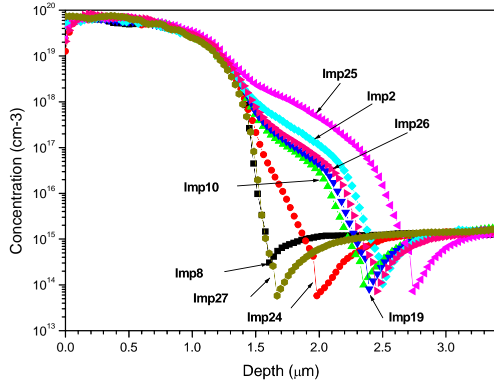

Fig. 2. Measured $N_{c\text{-}SRP}(x)$ profiles for samples showing different levels of ^{31}P cross-contamination.

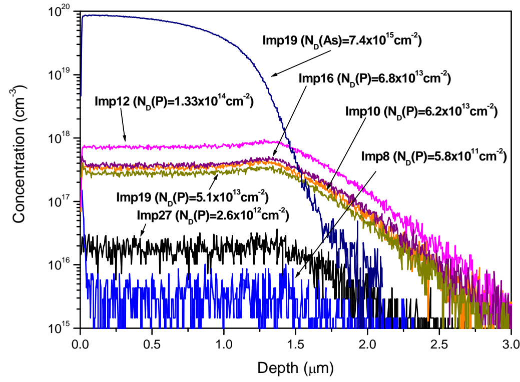

Fig.3. Selected SIMS $N_d(x)$ profiles measured after diffusion for samples showing different levels of ^{31}P cross-contamination in arsenic implantation.

SIMULATIONS

For simulation of phosphorus contamination in arsenic implantation we used the process simulator SUPREM-IV (S4). Experimental data from SIMS and SRP were used to calibrate the model. Diffusivities of arsenic and phosphorus were adjusted to better match SIMS and SRP results. Phosphorus contamination was simulated as additional implantation of phosphorus at implantation energy E=10 keV. Phosphorus contamination ranging from N_D= 1×10^{11} cm^{-2} up to N_D=4×10^{14} cm^{-2} was simulated. Simulated doping concentration profiles ($N_{Dt}(x)$ profiles) are shown in Fig. 4.

To be able to compare the simulated data with measured $N_{c\text{-}SRP}(x)$ profiles we have used an algorithm for calculation of on-bevel carrier concentration profile ($N_{c\text{-}bevel}(x)$ profile) that corresponds to $N_{c\text{-}SRP}(x)$ profile. For this calculation we used the algorithm described in [6]. This is a basic correction of the carrier spilling effect which shifts on-bevel *p-n* junction depth compared to the junction depth in a non-bevelled structure. Detailed discussion on SRP technique and the carrier spilling effect can be found in [7]. Calculated $N_{c\text{-}bevel}(x)$ profiles are shown in Fig. 5.

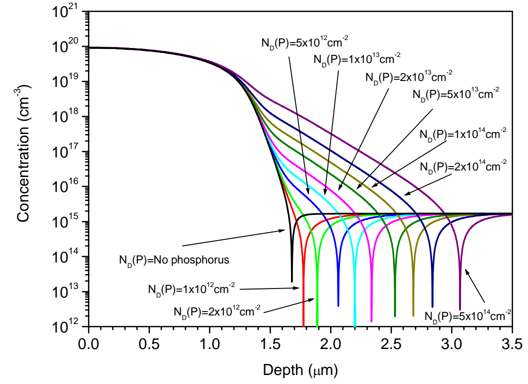

Fig. 4: Simulated $N_{dt}(x)$ profiles for different levels of phosphorus contamination.

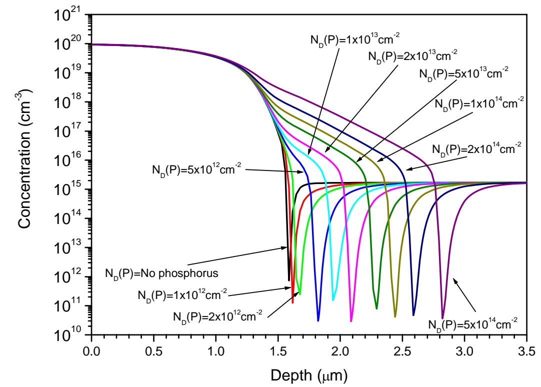

Fig. 5: Simulated cross-contaminated $N_{c\text{-}bevel}(x)$ profiles.

From these $N_{dt}(x)$ profiles and $N_{c\text{-}bevel}(x)$ profiles we have created a chart for conversion of ^{31}P cross-contamination dose to *p-n* junction depth (Fig. 6). This chart can be used to determine the level of contamination from $N_{c\text{-}SRP}(x)$ profiles for wide range of phosphorus cross-contamination doses from N_D(P)=1×10^{12} cm^{-2} to N_D(P)=1×10^{15} cm^{-2}.

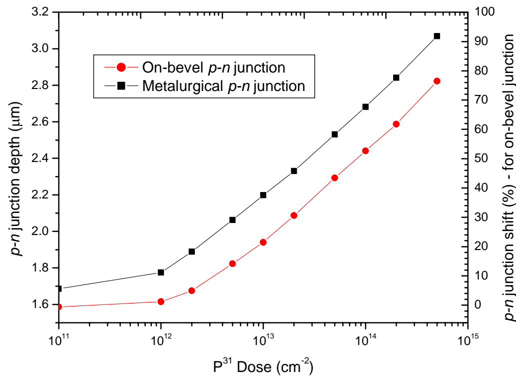

Fig. 6: Simulated dependence of *p-n* junction depth (metallurgical and on-bevel) for different levels of phosphorus contamination.

DISCUSSION

The results of our monitoring of the ion implanter for phosphorus contamination during arsenic implantation show that the levels of this contamination change in the course of implanter operation. The presence of phosphorus in arsenic implantation after the diffusion process results in a "phosphorus" tail in the carrier concentration profile, as shown in Fig. 2. This moves the *p-n* junction deeper in the substrate and could possibly degrade device performance. Phosphorus diffuses via a dual (vacancy and interstitially) mechanism, with the interstitially component dominating. Arsenic diffuses predominately via a vacancy mechanism that requires higher activation energies [8] and results in slower diffusion than phosphorus. Our method for determination of phosphorus contamination uses this difference in diffusivities between phosphorus and arsenic. As can be seen in Fig. 2 or from simulations (Fig. 4), with an increasing concentration of phosphorus also the shift increases of the *p-n* junction deeper into the substrate. By using a conversion chart from Fig. 6 we are able to determine the dose of ^{31}P from the depth of the *p-n* junction.

From our experimental results we can see that sample Imp8 has the *p-n* junction depth x_j=1.6 μm and according to Fig. 6 corresponds to N_D(P) < 1×10^{12} cm^{-2}, which is the detection limit for this technique. This sample Imp8 was implanted on an implanter not used for phosphorus implantations and therefore there should be no contamination present. The most significant shift of *p-n* junction was observed for sample Imp25 (x_j=2.75 μm) and corresponds to contamination N_D(P)=3.5×10^{14} cm^{-2}. From these results we can see that cross-contamination can result into *p-n* junction shift up to 1.15 micron (sample Imp25) that presents a 72% deeper junction. This shift of the *p-n* junction significantly influences the function of the integrated circuit.

To verify the simulated model we have created for determination of cross-contamination dose (Fig. 6) and to correlate the results to SIMS data we have compared the results of these two different techniques (SIMS, SRP). Some samples were measured by SIMS directly after implantation (Fig.1) and some samples were analyzed after diffusion by both techniques (SIMS, SRP) (Fig.3, Fig.2). These results are shown in Fig. 7. Both results after diffusion process (SIMS and SRP) are well matched. For samples that were measured immediately after implantation we can see a significantly lower dose of the measured phosphorus dose. However, these samples also seem to be tracking the trend of cross-contamination as for samples measured after diffusion. This difference between SIMS results could possibly be explained by the fact that after implantation most phosphorus is concentrated on the wafer surface and SIMS is not able to measure it correctly. Due to the diffusion process the phosphorus from the surface diffuses into silicon and thus is detected by SIMS after the diffusion process. This could explain why SIMS after diffusion shows almost the same cross-contamination values as SRP technique.

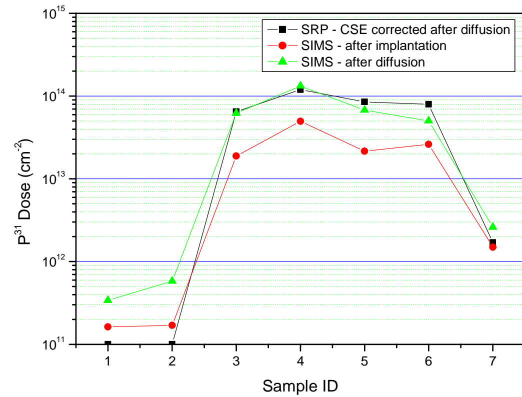

Fig. 7. Comparison of P^{31} cross-contamination results measured by SIMS (after implantation and after drive) and results determined using SRP method.

In our experiments we have also tested use of sacrificial oxide layer (22nm thick) that is being used to prevent contamination from reaching the silicon. As phosphorus is being co-implanted with significantly lower energy than arsenic, is should be trapped in this oxide layer. We have implanted wafer with oxide layer and wafer without any oxide in the same run. For comparison we have also taken the sample implanted on our other implanter that is not being used for implantation of phosphorus and should be practically phosphorus free. After diffusion process we have measured $N_{c\text{-}SRP}$(x) profiles and these are shown on Fig.8.

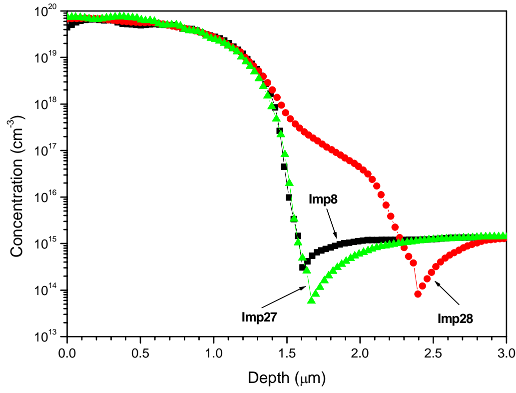

Fig.8. Comparison of $N_{c\text{-}SRP}$(x) profiles for samples implanted with oxide 22nm (Impl27), without oxide (Impl28) and on different implanter not used for phosphorus implantations (Impl8).

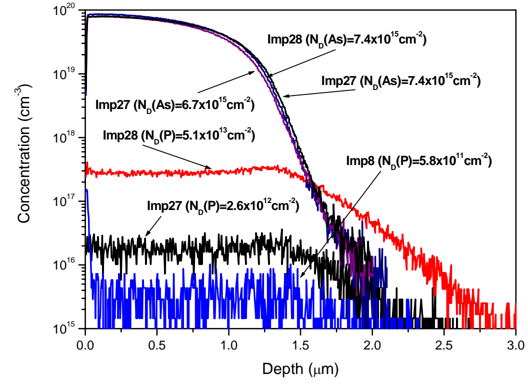

Fig.9. Comparison of N_d(x) profiles measured by SIMS for samples implanted with oxide 22nm (Impl27), without oxide (Impl28) and on different implanter not used for phosphorus implantations (Impl8).

As can be seen from Fig.8 reference sample Imp8 has *p-n* junction depth x_j=1.6µm, sample Imp27 implanted with the use of oxide layer shows *p-n* junction depth x_j=1.65µm and sample Imp28 implanted without any oxide layer shows *p-n* junction depth x_j=2.4µm. When we use conversion chart on Fig.6 we can estimate levels of phosphorus contamination for these samples. For sample Imp8 the phosphorus dose is less than $1x10^{12}cm^{-2}$. For sample Imp27 we can see small shift in *p-n* junction depth and significantly wider depletion region near the *p-n* junction is observed compared to Imp8. Estimated level of phosphorus in this case is approximately $N_D(P)$ = $2x10^{12}cm^{-2}$. Much worse situation is for sample Imp28 where we can see that *p-n* junction is shifted to x_j=2.4µm that corresponds to phosphorus cross-contamination dose $N_D(P)$ = $8x10^{13}cm^{-2}$. Results from this experiment show that thin oxide layer significantly reduces contamination in the silicon, however in this case was not able to reduce the contamination under detection limit of this method. This also shows that even when there is protection oxide layer used to prevent contamination it can not fully eliminate the contamination and levels of contamination should be regularly monitored. To verify the results from SRP analysis we have used SIMS to confirm these results (Fig.9). As can be seen SIMS results confirmed our results obtained by SRP, showing highest phosphorus for sample Imp28 ($N_D(P)$ = $5.3x10^{13}cm^{-2}$), less for sample Imp28 with screen oxide ($N_D(P)$ = $2.6x10^{12}cm^{-2}$) and less than $1x10^{12}cm^{-2}$ phosphorus contamination for sample Imp8($N_D(P)$ = $5.8x10^{11}cm^{-2}$). Dose of implanted arsenic is the same for samples Imp8 and Imp28 but sample with oxide shows lower dose due to part of the arsenic dose lost in the oxide.

The accuracy of our method using SRP depends on several factors. One of the critical factors is how simulation matches the real process. In this case we have tuned the simulator to match the results and to improve the preciseness of this method we have also calculated the on-bevel carrier concentration profiles that are measured by SRP. Another important factor is the preciseness of *p-n* junction depth measurement. The accuracy of the doping concentration $N_c(x)$ determination is ±10% and the depth of the *p-n* junction could be determined with accuracy ±5% by SRP method [9, 10]. The $N_D(x)$ profile of implanted phosphorus and antimony layers can be measured by SIMS with accuracy ±10%. Next factor influencing the results is substrate concentration because this can affect the junction depth, however, it is quite simple to apply correction for substrate carrier concentration. Another factor is repeatability of the diffusion process (temperature profile), however, this usually does not present an issue.

In our case we can see that the contamination can reach doses up to 3×10^{14} cm^{-2} of co-implanted phosphorus (sample IMP25) and corresponds to almost 3.8% of the implanted dose. Our monitoring has shown that the cross-contamination can vary extremely and that is the reason why it needs to be monitored regularly. We have implemented monitoring of our implanters on weekly bases by SRP measurements. This method is much faster than SIMS and also less expensive. It can detect the doses of ^{31}P as low as 1×10^{12} cm^{-2}. This limit is sufficient because a lower cross-contamination dose does not significantly affect the final doping profiles and does not affect the device function.

CONCLUSION

We have presented an alternative method for monitoring of ^{31}P cross-contamination for ^{75}As implantation using simulations and SRP measurements. Our method is based on the difference in diffusion between arsenic and phosphorus and uses the *p-n* junction depth as indication of the level of phosphorus cross-contamination. For measurement of the *p-n* junction depth we used the spreading resistance profiling technique. A simulation model for different levels of phosphorus contamination (N_D(P)=1×10^{11} cm^{-2} to N_D(P)=4×10^{14} cm^{-2}) in arsenic implantation was calculated showing the impact upon $N_{dt}(x)$ profiles (Fig. 4). To allow correct comparison we calculated also theoretical $N_{c\text{-}bevel}(x)$ profiles (Fig.5) that better match real $N_{c\text{-}SRP}(x)$ profiles.
Experimental data from several implanter runs were collected and analysed by SIMS (Fig. 1,Fig. 3) and SRP (Fig. 2) showing different levels of phosphorus contamination present in arsenic implantation and its effect on $N_{c\text{-}SRP}(x)$ profile. We have shown that cross-contamination can result into *p-n* junction shift up to 1.15 micron that presents a 72% deeper junction. From the results we can see that SIMS analysis directly after implantation shows a significantly lower dose of phosphorus that is present on the wafer and is seen after diffusion process (by both SIMS and SRP). These data have shown that SIMS measurement of dose of co-implanted phosphorus can be significantly underestimated when measured directly after implantation. Good correlation has been found between SIMS and SRP results after diffusion process (Fig. 7). This confirms that SRP technique presents another easy possibility for monitoring ^{31}P cross-contamination and can be used for in-line implanter monitoring. We have also studied effect of use of sacrificial oxide layer (22nm thick) to prevent the contamination. This oxide layer has shown to significantly reduce the contamination in the substrate however did not eliminate it completely. This is reason why it is necessary to control the level of cross-contamination.

ACKNOWLEDGEMENTS

This work was supported by a grant of the Slovak Grant Agency Vega No. 1/3111/06 and by project APVV-20-055405.

REFERENCES

[1] – R.B. Fair and W.G.Meyer, “Modeling Anomalous Junction Formation in Silicon by the Codiffusion of Implanted Arseni with Phosphorus,” ASTM STP 804, ed. D.C.Gupta, ASTM, 1983, pp.290-305

[2] – S.S. Todorov, A.Bertuch, W. Piscitello, R.Eddy, T.Robertson, “Advances in Cross-Contamination Control Using Single-Wafer, High-Current Implantation”, Ion Implantation Technology, 2000. Conference on, 2000, pp.715 – 718

[3] – Michael T.Wauk, A. Murrell, D. Wagner, P. Edwards, “Mechanism of Elemental Contamination in Ion Implantation Equipment”, Ion Implantation Technology. Proceedings of the 11th International Conference , Jun, 1996, pp.117-120

[4] – M. Kuruc, L. Hulényi, R. Kinder, “Determination of phosphorus contamination during antimony implantation by measurement and simulation”, Applied Surface Science, 2006

[5] – M. Kuruc, L. Hulényi, R. Kinder, A. Vincze, “Analysis and prevention of phosphorus contamination during antimony implantation”, Journal of Electrical Engineering, Vol. 56, 2005

[6] – M. Kuruc, L. Hulényi, R. Kinder, “Simulation of Carrier Spilling Effect for Bevelled Structures“, Proc. of 12th International Workshop on Applied Physics of Condensed Matter, 2007

[7] – T.Clarysse, V. Vanhaeren, I. Hoflijk, W. Vandervorst, „Characterization of electrically active dopant profiles with the spreading resistance probe“, Materials Science & Engineering, Volume 47, Issues 5-6, December 2004

[8] – SZE et al., VLSI Technology (Second Edition), McGraw-Hill International editions, 1988

[9] - M.I. Current, C.B. Yarling, Materials and Characterization of Ion Implantation, Ion Beam Press, 1997

[10] - SSM BAM (Bevel Angle Measurement), rev.1.2, Technical Data Sheet, Solid State Measurements, Inc., July 2002